Preprints are preliminary reports that have not undergone peer review.
They should not be considered conclusive, used to inform clinical practice,
or referenced by the media as validated information.

New Technique for Detecting Cracked Teeth and Evaluating the Crack Depth by Contrast-enhanced Cone Beam Computed Tomography: an in Vitro Study

Jie Zhou
Wuqing People Hospital
Jieni Fu
Hangzhou stomatological hospital
Mo Xiao
Tianjin Medical University
Yangyang Lv
Wuxi Stomatology Hospital
Fei Wu
Yantai Stomatological Hospital Affiliated to Binzhou Medical College
Feng Qiao
Tianjin Medical University
Tiantian Fu
Tianjin Medical University
Cuicui Sun
Tianjin Stomatological Hospital
Peng Li
Tianjin Medical University
Ligeng Wu (lwu06@tmu.edu.cn)
Tianjin Medical University

Research Article

Keywords: Cracked teeth, Cone beam computed tomography, Micro-computed tomography, Periapical radiography, crack depths

Posted Date: December 1st, 2021

DOI: https://doi.org/10.21203/rs.3.rs-1110699/v1

License: This work is licensed under a Creative Commons Attribution 4.0 International License.
Read Full License

Abstract

Background: Develop a new technique based on contrast-enhanced cone beam computed tomography (CBCT) to improve the detection of cracked teeth and the accuracy of crack depth evaluation in vitro.

Methods: We developed an in vitro artificial simulation model of cracked teeth. Pre-experimental CBCT (pre-CBCT), and micro-computed tomography (micro-CT) were first performed for all cracked teeth (n = 31). Contrast-enhanced CBCT was then performed by infiltrating the crack with ioversol under vacuum conditions. The results of pre-CBCT, micro-CT, and contrast-enhanced CBCT were recorded. SPSS v.26.0 software (IBM Corp, Somers, NY) and R software , version 3.6.0 (R Foundation for Statistical Computing; http://www.r-project.org/) and RStudio 1.1.[46]3 (RStudio, PBC, Boston, MA, US) were used to perform the statistical analysis for the study.

Results: The sensitivities of pre-CBCT and contrast-enhanced CBCT were 48.4%, and 67.7%, respectively. ICC value of crack depth as measured by pre-CBCT and contrast-enhanced CBCT was 0.847 (95% confidence interval:0.380-0.960; $P < 0.001$). The areas under ROC curves (AUC) of pre-CBCT and contrast-enhanced CBCT were different, the AUC of pre-CBCT was 0.958 ($P = 0.000$, 95% CI :0.843-1.074), and the AUC of enhanced CBCT was 0.979 ($P = 0.000$, 95% CI :0.921-1.037), and the difference was not statistically significant (Z=-0.707, $P = 0.480$). The ICC value of crack depth as measured by contrast-enhanced CBCT and micro-CT was 0.753 (95% CI: 0.248-0.911; $P < 0.001$).

Conclusion: Contrast-enhanced CBCT under vacuum conditions with a contrast medium can only significantly improve the cracks detection rate of cracked teeth, but not measure the crack depths accurately.

Background

Cracked teeth extend from the crown toward the apex and gradually propagate into the dentin, involving one or two marginal ridges[1, 2]. Cracked teeth may produce variable clinical symptoms depending on the extension depth of the crack and subsequent bacterial infections[3]. The typical symptoms are unexplained pain when exposed to a cold stimulus and sharp pain during chewing or releasing[4]. Sometimes, a narrow and deep periodontal pocket indicates that the crack extends subgingivally[5, 6].

There are several auxiliary approaches for diagnosing cracked teeth, including operating microscopes[7, 8], transillumination[9–11], methylene blue staining[9], and the Tooth Slooth[12]. In addition, quantitative percussion diagnosis[13] and direct supra-coronal splinting[14] have proven equally effective in a clinical setting. However, techniques to reliably determine the extension depths of cracked teeth before treatment are lacking.

Many studies have investigated the diagnosis and depth assessment of cracked teeth in vitro. Imai et al.[15–19] reported that optical coherence tomography (OCT) was effective in detecting cracks. OCT could effectively detect enamel cracks within 3 mm of depth but could not diagnose structural cracks that caused clinical symptoms. Jun et al.[20, 21]used, for the first time, quantitative laser-induced fluorescence (QLF) to detect tooth cracks; however, QLF could only diagnose enamel cracks. Matsushita–Tokugawa[22] used infrared thermography to detect cracked teeth. This technique could detect cracks with a width of only 4–35.5 μm, but its performance was limited when the width exceeded 42 μm.

Radiological examination, such as cone beam computed tomography (CBCT), is a commonly used diagnostic tool, but can only be used to diagnose wide cracks[23, 24]. Additionally, such examination is usually applied to diagnose vertical root fractures (VRFs)[25–28]. A few studies have reported the efficiency of magnetic resonance imaging (MRI) in diagnosing cracked teeth, but the reliability of MRI in vivo has not been confirmed[29, 30]. Micro-computed tomography (micro-CT) has high resolution and is commonly considered the gold standard diagnostic approach for detecting microcracks in vitro[31]. An in vitro study confirmed that infiltrating the crack with the contrast agent barium sulfate and then performing contrast-enhanced micro-CT can produce high-density linear images of fine cracks on the radiographs[32]. Therefore, the detection of fine cracks can be improved using micro-CT, and the crack invasion depth can be calculated; however, it can only be used in ex vivo experiments. Although the resolution of CBCT is not as good as that of micro-CT, it can be used in patients; hence, the diagnostic applicability of CBCT in clinical settings needs to be improved.

In this study, in order to improve CBCT as a tool to determine the crack depth of cracked teeth before treatment, we aimed to explore a technique based on contrast-enhanced CBCT, and asked whether it would predict the crack depth of cracked teeth.

Methods

From January to December 2018, we collected 200 intact teeth extracted by minimally invasive techniques for periodontal or orthodontic reasons at the Department of Oral and Maxillofacial Surgery, Stomatological Hospital of Tianjin Medical University. This study was approved by the ethics committee of the Stomatological Hospital of Tianjin Medical University (TMUhMEC2019014). The inclusion criterion was the absence of enamel cracks visible with the naked eye. The exclusion criteria were the presence of dental caries, wedge-shaped defects, and VRFs, and a previous history of root canal therapy or restoration. Finally, 40 teeth that met the criteria were screened in vitro.

All the 40 screened intact teeth were cleaned to remove soft tissue and calculus, and soaked in 0.1% thymol solution for 24 hours. Then they were placed in 0.9% saline solution, soaked in liquid nitrogen (-196°C) for 1 min and immediately transferred into hot water (90°C) for 5 min[23, 33]. The teeth were then observed under a surgical operating microscope (OMS2350; Zumax, Suzhou, China) under 17× magnification. Among the 40 teeth, 31 were selected as artificially cracked teeth, as they had a structural crack visible under this magnification; the remaining 9 teeth were excluded due to splits or absence of cracks.

The 31 cracked teeth were randomly embedded in four trays, and the root portion of each tooth was wrapped in wax to simulate the periodontal tissue before performing pre-CBCT (Kavo 3D exam, Germany).

The pre-CBCT parameters were as follows: voltage, 120 kV; current, 8 mA; matrix size, 640 x 640; field of view, 8 × 8 cm; and pixel size, 0.125 mm × 0.125 mm. To ensure better pre-CBCT imaging quality, the operations were performed by a technician. The pre-CBCT results were stored in a database, and pre-CBCT images were analyzed using the Vision Q (KaVoeXam Vision) software package.

To accurately evaluate the crack depth of the 31 cracked teeth, micro-CT (SIEMENS, Munich, Germany), considered the gold standard, was performed. The micro-CT parameters were as follows: voltage, 80 KV; current, 500 μA; resolution, 9.08 μm; exposure time, 1000 ms.Inveon Research Workplace software (SIEMENS, Munich, Germany) was used to reconstruct three-dimensional images. The presence of cracks and their extension depths, as measured from the micro-CT images, was recorded by a radiologist who was blinded to the evaluation of pre-CBCT images.

The procedure to measure crack depth extending from the crown to the root on micro-CT images(Fig. 1A-C) was as follows: The cracked tooth was adjusted to keep it upright in the coronal and sagittal planes; then, the cracks were observed from the crown to the root in the horizontal plane. When the crack appeared in the crown for the first time on the horizontal plane, the layer was recorded as “a”; the crack was observed extending to the root, always on the horizontal plane. When the crack began to disappear on the root, the layer was recorded as “b”; the distance from “a” to “b,” measured with the ruler tool, was considered the crack depth.

Ioversol solution ($C_{18}H_{24}I_3N_3O_9$; Hengrui Pharmaceutical, Jiangsu, China) was diluted at a ratio of 3:1 in normal saline to increase its fluidity. The crown and root of each cracked tooth were isolated with a rubber dam, and the crown was filled with the diluted ioversol solution. The teeth and the rubber dam were kept in place using a rubber band and a paper cup(Fig. 2A). The teeth were placed in a closed glass jar, connected to the suction pump with a rubber tube (Fig. 2B). Negative pressure was applied gradually until it reached -0.08 MPa and was maintained at this value for 1 min. Then, normal atmospheric pressure was restored. This procedure was repeated once again. The teeth were then removed from the jar. The crack was infiltrated with ioversol under vacuum conditions throughout the procedure.After infiltration, the cracked teeth remained in the trays with wax and underwent contrast-enhanced CBCT with the same parameters as used for pre-CBCT.

Two observers, an endodontic graduate student and an experienced radiologist, were involved the evaluation. Before the study, the two observers were trained to achieve a high degree of consistency. Then, the presence and absence of cracks were determined using pre-CBCT and contrast-enhanced CBCT by the two observers. In the event of disagreement among the observers, the image was re-examined until a consensus was reached. The following 2-point rating scale was used to determine whether cracks were present on pre-CBCT: (i) probably or definitely not a lesion, (ii) probably or definitely a lesion.

On contrast-enhanced CBCT, a high-density linear crack was considered to mark a cracked tooth (Fig. 4C). The method used for measuring cracks on contrast-enhanced CBCT was the same as that used for micro-

CT(Fig. 3A-E) : The position of the tooth was adjusted in the sagittal and coronal planes to keep it upright; the cracks were observed from the crown to the root on the horizontal plane. When the high-density crack appeared in the crown for the first time on the horizontal plane, a horizontal line was marked as “1” in the coronal plane with the "distance" tool, indicating the level of the first occurrence of the crack. The crack was observed extending to the root, always on the horizontal plane. When the high-density crack disappeared completely, the layer was marked as “2” in the coronal plane; this represented the apical point of the crack. The "distance" tool was used to draw a vertical line from 1 to 2 in the coronal plane, and this was marked as “3,” representing the crack depth as measured by contrast-enhanced CBCT. The extension depth of the cracked teeth on the contrast-enhanced CBCT was measured by the radiologist. Each crack depth value was measured three times at one-week intervals by the same radiologist, and the average value was considered as the final crack depth.

SPSS v.26.0 software (IBM Corp, Somers, NY) and R software, version 3.6.0 (R Foundation for Statistical Computing; http://www.r-project.org/) and RStudio 1.1.[46]3 (RStudio, PBC, Boston, MA, US) were used to perform the statistical analysis for the study.

The K-means clustering algorithm was first published in 1955 and is still widely used despite having been proposed over 50 years ago even though thousands of clustering algorithms have been published since then[34]. It is undoubtedly the most widely used partitional clustering algorithm[35]. Crack depths measured by micro-CT were transformed into categorical variables according to the K-means clusters.

For further analysis, the Bland-Altman plot was used to analyze the consistency of the crack depths between pre-CBCT and contrast-enhanced CBCT. The intraclass correlation coefficient (ICC) was used to evaluate the consistency of the crack depths as measured on pre-CBCT and contrast-enhanced CBCT, as well as between contrast-enhanced CBCT and micro-CT. Receiver operating characteristic (ROC) curves were generated to assess the ability to predict cracked teeth in the differential diagnosis using contrast-enhanced CBCT and micro-CT.

Moreover, restricted cubic splines were also with 4 knots at the 5th, 35th, 65th, and 95th percentiles to model the non-linear relationship between the crack depths of contrast-enhanced CBCT and those of micro-CT.

Results

The results of pre-CBCT, micro-CT, and contrast-enhanced CBCT were recorded(Fig. 4A-C).Thirty-one cracked teeth generated by the artificial simulation model were included in this study. Only 15 cracked teeth could be identified using pre-CBCT, whereas 21 could be identified using contrast-enhanced CBCT ,and 11 could be identified using both pre-CBCT and contrast-enhanced CBCT.(Fig. 5A).

The sensitivity values of pre-CBCT and contrast-enhanced CBCT for diagnosing cracked teeth were 48.4%, and 67.7%, respectively, implying that the sensitivity of contrast-enhanced CBCT was found to be higher than that of pre-CBCT(Fig. 5B).

The mean crack depth of the 10 teeth that were only measured on contrast-enhanced CBCT, but not visible on pre-CBCT was 7.114 ± 1.587 mm. Meanwhile, the mean crack depth of the 4 cracked teeth detected only during pre-CBCT, and not contrast-enhanced CBCT, was 7.2650 ± 1.135 mm.

The K-means clustering algorithms was used to transform the crack depths measured by micro-CT from continuous variables into 2 categories, defined as deep cracks and shallow cracks.The ICC value of crack depth, measured by pre-CBCT and contrast-enhanced CBCT, was 0.847 (95% confidence interval [CI]: 0.380-0.960; $P < 0.001$), demonstrating strong consistency. Both pre-CBCT and contrast-enhanced CBCT exhibited good consistency in determining crack depth (Fig. 6).

The areas under the ROC curves (AUC) of pre-CBCT is 0.958 ($P < 0.001$, 95% CI: 0.843-1.074), and that contrast-enhanced CBCT is 0.979 ($P = 0.000$, 95% CI: 0.921-1.037). The AUCs of pre- and contrast-enhanced CBCT were different; however, the difference was not statistically significant (Z = -0.707, $P = 0.480$; Fig. 7).

The ICC value of crack depth, as measured by contrast-enhanced CBCT and micro-CT, was 0.753 (95% CI: 0.248-0.911; $P < 0.001$), demonstrating strong consistency. Contrast-enhanced CBCT can explain 72.36% of the micro-CT changes, and the root mean square error (RMSE) was only 1.81. We observed a linear relationship between the crack depths measured by contrast-enhanced CBCT and micro-CT(Fig. 8).

Discussion

Methylene blue staining[7, 9] of the tooth surface can help in the visualization of cracks, but not in the measurement of their depth. In this study, ioversol solution was used as a crack indicator via infiltration of the crack under vacuum conditions to obtain a high-density linear image using CBCT, thus allowing for contrast-enhanced CBCT and observation of the crack. Ioversol is a nonionic contrast agent, often used in angiography of the cerebral artery, coronary artery, and peripheral artery, as well as in other types of angiography[36, 37]. It helps obtain high-density images by radiography, thus allowing clear imaging of the vascular path. In this study, it was used as a "dye" to explore whether it can display cracks on contrast-enhanced CBCT images.

Our results indicate that more cracked teeth can be detected using contrast-enhanced CBCT, because the diagnostic sensitivity of cracked teeth in an artificial simulation model with contrast-enhanced CBCT was considerably higher than that with pre-CBCT. The X-ray photons passing through a radiolucent fracture plane also pass through extensive amounts of radiopaque healthy tooth structure; thus, tooth cracks may not be apparent[38]. Therefore, if measures were taken to make the crack image show higher density than healthy structure, it is more likely that it will not be masked by healthy tooth structure. Ioversol as a medium enables high-resolution morphological assessment of articular cartilage in small animals using CBCT[39]. It has been inferred that ioversol could be used in hard tissue imaging to enhance diagnostic ability. A recent study has shown that contrast-enhanced CBCT using meglumine iatrizoate as medium can show more cracked lines[40].

The fact that the 4 teeth detected only by pre-CBCT had a greater mean crack depth than that of the 10 teeth only observable on contrast-enhanced CBCT might be explained by the following: (i) The crack direction of the artificial model in this study is uncertain, making ioversol infiltration difficult; (ii) the crack depth in the present study was not controlled, and the above two sets of data are not comparable.

Our study revealed no significant differences between pre-CBCT and contrast-enhanced CBCT in measuring the crack depth of cracked teeth. This may be because crack width may impact the diagnostic accuracy of CBCT in detecting cracked teeth[41–43]. If the crack is wide, the results of pre-CBCT and contrast-enhanced CBCT may not differ significantly. However, when the crack is narrow, it may not be clearly visible during pre-CBCT, but can be seen more clearly on contrast-enhanced CBCT when ioversol is used as a medium. Therefore, when cracks can definitively be detected on pre-CBCT, their depths (when measured using pre-CBCT) are very close to those measured using contrast-enhanced CBCT.

Furthermore, the crack depths measured on contrast-enhanced CBCT and micro-CT demonstrated good consistency. The result of restricted cubic splines (RCS) showed the relationship between the difference in the crack depths measured on contrast-enhanced CBCT and micro-CT to be linear. However, a formula cannot be obtained to calculate the specific relationship between the depth measured by contrast-enhanced CBCT and micro-CT.

It is worth mentioning that the crack depth measured by both micro-CT and contrast-enhanced CBCT was a vertical distance from the crown to root, i.e., it was not the actual length of the crack. Considering that most cracks were oblique, it was difficult to access the section that was exactly the full length of the crack in a plane. Additionally, the vertical distance of the crack depth from the crown to the root can better represent the degree of damage to the full length of the tooth.

There are some limitations to our study:(i) the sample size was small, as 31 artificially cracked teeth were analyzed in our study; however, in order to analyze the relationships between the crack depths measured by contrast-enhanced CBCT and micro-CT, only 21 teeth detected as cracked by both technologies were statistically analyzed. The result needs to be further confirmed using a larger sample size;(ii) the study was conducted in vitro; thus, the feasibility of the clinical application of this technique needs to be confirmed in the future; (iii) the artificial model of cracked teeth was somewhat random; therefore, its width should be considered in future studies, if possible.

We conducted the study and aimed to develop a new technique based on CBCT to improve the detection of cracked teeth and the accuracy of crack depth evaluation in vitro.The study suggests that CBCT with a high-density contrast medium is reliable for detecting cracks. On the basis of our findings, simulated animal experiments in controlled negative pressure conditions are warranted. If it is viable, we resolved the scientific problem.

Conclusion

Contrast-enhanced CBCT under vacuum conditions with a contrast medium can significantly improve the crack detection rate of cracked teeth, but cannot measure the crack depth accurately.

Abbreviations

CBCT: cone beam computed tomography; pre-CBCT: Pre-experimental CBCT; micro-CT: micro-computed tomography; OCT: optical coherence tomography; QLF: quantitative laser-induced fluorescence; VRFs: vertical root fractures; MRI: magnetic resonance imaging; ICC: The intraclass correlation coefficient; ROC: Receiver operatingcharacteristic; AUC: The areas under the ROC curves; RMSE: the root mean square error.

Declarations

Acknowledgements

None.

Authors' contributions

JZ, JF,and MX conducted the experiment throughout the study was involved in drafing and revising the manuscript. YLv and FW were responsible for cases collection.FQ, TTF and CCS was responsible for statistical analysis. PL was responsible for project administration.LW designed and supervised the research. All authors read and approved the final manuscript.

Funding

This work was supported by the Development of Science and Technology Plan Projects of Wu Qing District, Tianjin (grant number WQKJ201728 and WQKJ202133); Scientific Research Program of Tianjin Education Commission, China (grant number 2020KJ184).

Availability of data and materials

The datasets used and/or analysed during the current study are available from the corresponding author on reasonable request.

Ethics approval and consent to participate

This study was approved by the ethics committee of the Stomatological Hospital of Tianjin Medical University (TMUhMEC2019014). Informed consents were obtained from all subjects.

Consent for publication

All data published here are under the consent for publication.

Competing interests

The authors confirm that they have no conflict of interest.

References

1. Kahler W. The cracked tooth conundrum: terminology, classification, diagnosis, and management. Am J Dent. 2008; 21:275-82.
2. Denis E, Simon III. Cracking the cracked tooth code. Endo. 1997; (fall/winter):1-13.
3. Ricucci D, Siqueira JF, Loghin S, Berman LH. The cracked tooth: histopathologic and histobacteriologic aspects. J Endod. 2015; 41:343-52.
4. Hilton TJ, Funkhouser E, Ferracane JL et al. Associations of types of pain with crack-level, tooth-level and patient-level characteristics in posterior teeth with visible cracks: Findings from the National Dental Practice-Based Research Network. J Dent. 2018; 70:67-73.
5. Kang SH, Kim BS, Kim Y. Cracked teeth: distribution, characteristics, and survival after root canal treatment. J Endod. 2016; 42:557-62.
6. Yang SE, Jo AR, Lee HJ, Kim SY. Analysis of the characteristics of cracked teeth and evaluation of pulp status according to periodontal probing depth. BMC oral health. 2017; 17:135.
7. Clark DJ, Sheets CG, Paquette JM. Definitive diagnosis of early enamel and dentin cracks based on microscopic evaluation. J Esthet Restor Dent. 2003; 15:391-401.
8. Slaton CC, Loushine RJ, Weller RN et al. Identification of Resected Root-end Dentinal Cracks: A Comparative Study of Visual Magnification. J Endod. 2003; 29:519-22.
9. Wright HM, Loushine RJ, Weller RN, Kimbrough WF, Pashley DH. Identification of resected root-end dentinal cracks: a comparative study of transillumination and dyes. J Endod. 2004; 30:702-15.
10. Oliveira LRS, Braga SSL, Bicalho AA et al. Molar cusp deformation evaluated by micro-CT and enamel crack formation to compare incremental and bulk-filling techniques. J Dent. 2018; 74:71-8.
11. Liewehr FR. An inexpensive device for transillumination. J Endod. 2001; 27:130-1.
12. Yang Y, Chen G, Hua F, Yu Q, Yang W. Biting pain reproduced by the tooth slooth: an aid for early diagnosis of cracked tooth. Quintessence Int. 2019; 50:82-7.
13. Sheets CG, Wu JC, Rashad S, Phelan M, Earthman JC. In vivo study of the effectiveness of quantitative percussion diagnostics as an indicator of the level of the structural pathology of teeth. J Prosthet Dent. 2016; 116:191-9.e1.
14. Banerji S, Mehta SB, Kamran T, Kalakonda M, Millar BJ. A multi-centred clinical audit to describe the efficacy of direct supra-coronal splinting–a minimally invasive approach to the management of cracked tooth syndrome. J Dent. 2014; 42:862-71.
15. Imai K, Shimada Y, Sadr A, Sumi Y, Tagami J. Noninvasive cross-sectional visualization of enamel cracks by optical coherence tomography in vitro. J Endod. 2012; 38:1269-74.
16. Lee SH, Lee JJ, Chung HJ, Park JT, Kim HJ. Dental optical coherence tomography: new potential diagnostic system for cracked-tooth syndrome. Surg Radiol Anat. 2016; 38:49-54.

17. Segarra MS, Shimada Y, Sadr A, Sumi Y, Tagami J. Three-Dimensional Analysis of Enamel Crack Behavior Using Optical Coherence Tomography. J Dent Res. 2017; 96:308-14.
18. De Oliveira BP, Câmara AC, Duarte DA et al. Detection of Apical Root Cracks Using Spectral Domain and Swept-source Optical Coherence Tomography. J Endod. 2017; 43:1148-51.
19. Nakajima Y, Shimada Y, Miyashin M et al. Noninvasive cross-sectional imaging of incomplete crown fractures (cracks) using swept-source optical coherence tomography. Int Endod J. 2012; 45:933-41.
20. Jun MK, Ku HM, Kim E et al. Detection and Analysis of Enamel Cracks by Quantitative Light-induced Fluorescence Technology. J Endod. 2016; 42:500-4.
21. Jun MK, Park SW, Lee ES, Kim BR, Kim BI. Diagnosis and management of cracked tooth by quantitative light-induced fluorescence technology. Photodiagnosis Photodyn Ther. 2019; 26:324-6.
22. Matsushita-Tokugawa M, Miura J, Iwami Y et al. Detection of dentinal microcracks using infrared thermography. J Endod. 2013; 39:88-91.
23. Wang S, Xu Y, Shen Z et al. The Extent of the Crack on Artificial Simulation Models with CBCT and Periapical Radiography. PLoS One. 2017; 12:e0169150.
24. Kalyan Chakravarthy PV, Telang LA, Nerali J, Telang A. Cracked tooth: a report of two cases and role of cone beam computed tomography in diagnosis. Case Rep Dent. 2012; 2012:525364.
25. Abdinian M, Razavian H, Jenabi N. In Vitro Comparison of Cone Beam Computed Tomography with Digital Periapical Radiography for Detection of Vertical Root Fracture in Posterior Teeth. J Dent (Shiraz). 2016; 17:84-90.
26. Edlund M, Nair MK, Nair UP. Detection of vertical root fractures by using cone-beam computed tomography: a clinical study. J Endod. 2011; 37:768-72.
27. Kositbowornchai S, Nuansakul R, Sikram S, Sinahawattana S, Saengmontri S. Root fracture detection: a comparison of direct digital radiography with conventional radiography. Dentomaxillofac Radiol. 2001; 30:106-9.
28. Hassan B, Metska ME, Ozok AR, Van Der Stelt P, Wesselink PR. Detection of vertical root fractures in endodontically treated teeth by a cone beam computed tomography scan. J Endod. 2009; 35:719-22.
29. Idiyatullin D, Garwood M, Gaalaas L, Nixdorf DR. Role of MRI for detecting micro cracks in teeth. Dentomaxillofac Radiol. 2016; 45:20160150.
30. Schuurmans TJ, Nixdorf DR, Idiyatullin DS et al. Accuracy and Reliability of Root Crack and Fracture Detection in Teeth Using Magnetic Resonance Imaging. J Endod. 2019; 45:750-5.e2.
31. De-Deus G, Belladonna FG, Silva E et al. Micro-CT assessment of dentinal micro-cracks after root canal filling procedures. Int Endod J. 2017; 50:895-901.
32. Landrigan MD, Flatley JC, Turnbull TL et al. Detection of dentinal cracks using contrast-enhanced micro-computed tomography. J Mech Behav Biomed. 2010; 3:223-7.
33. Lloyd BA, Mcginley MB, Brown WS. Thermal stress in teeth. J Dent Res. 1978; 57:571-82.
34. Jain AK. Data clustering: 50 years beyond K-means. Pattern Recognition Letters. 2009; 31:651-66.
35. Jain AK, Murty MN, Flynn PJ. Data Clustering: A Review. ACM Comput Surv. 1999; 31:264-323.

36. Fischbach R, Landwehr P, Svaland M et al. Spiral CT angiography of the abdominal aorta. comparison of iodixanol and ioversol. Invest Radiol. 1999; 34:374-80.
37. Nijhof WH, Baltussen EJ, Kant IM et al. Low-dose CT angiography of the abdominal aorta and reduced contrast medium volume: assessment of image quality and radiation dose. Clin Radiol. 2016; 71:64-73.
38. Mamoun JS, Napoletano D. Cracked tooth diagnosis and treatment: An alternative paradigm. Eur J Dent. 2015; 9:293-303.
39. Ter Voert CEM, Kour RYN, Van Teeffelen BCJ, Ansari N, Stok KS. Contrast-enhanced micro-computed tomography of articular cartilage morphology with ioversol and iomeprol. J Anat. 2020; 237:1062-71.
40. Yuan M, Gao AT, Wang TM et al. Using Meglumine Diatrizoate to improve the accuracy of diagnosis of cracked teeth on Cone-beam CT images. Int Endod J. 2020; 53:709-14.
41. Ozer SY. Detection of vertical root fractures of different thicknesses in endodontically enlarged teeth by cone beam computed tomography versus digital radiography. J Endod. 2010; 36:1245-9.
42. Makeeva IM, Byakova SF, Novozhilova NE et al. Detection of artificially induced vertical root fractures of different widths by cone beam computed tomography in vitro and in vivo. Int Endod J. 2016; 49:980-9.
43. Brady E, Mannocci F, Brown J, Wilson R, Patel S. A comparison of cone beam computed tomography and periapical radiography for the detection of vertical root fractures in nonendodontically treated teeth. Int Endod J. 2014; 47:735-46.

Figures

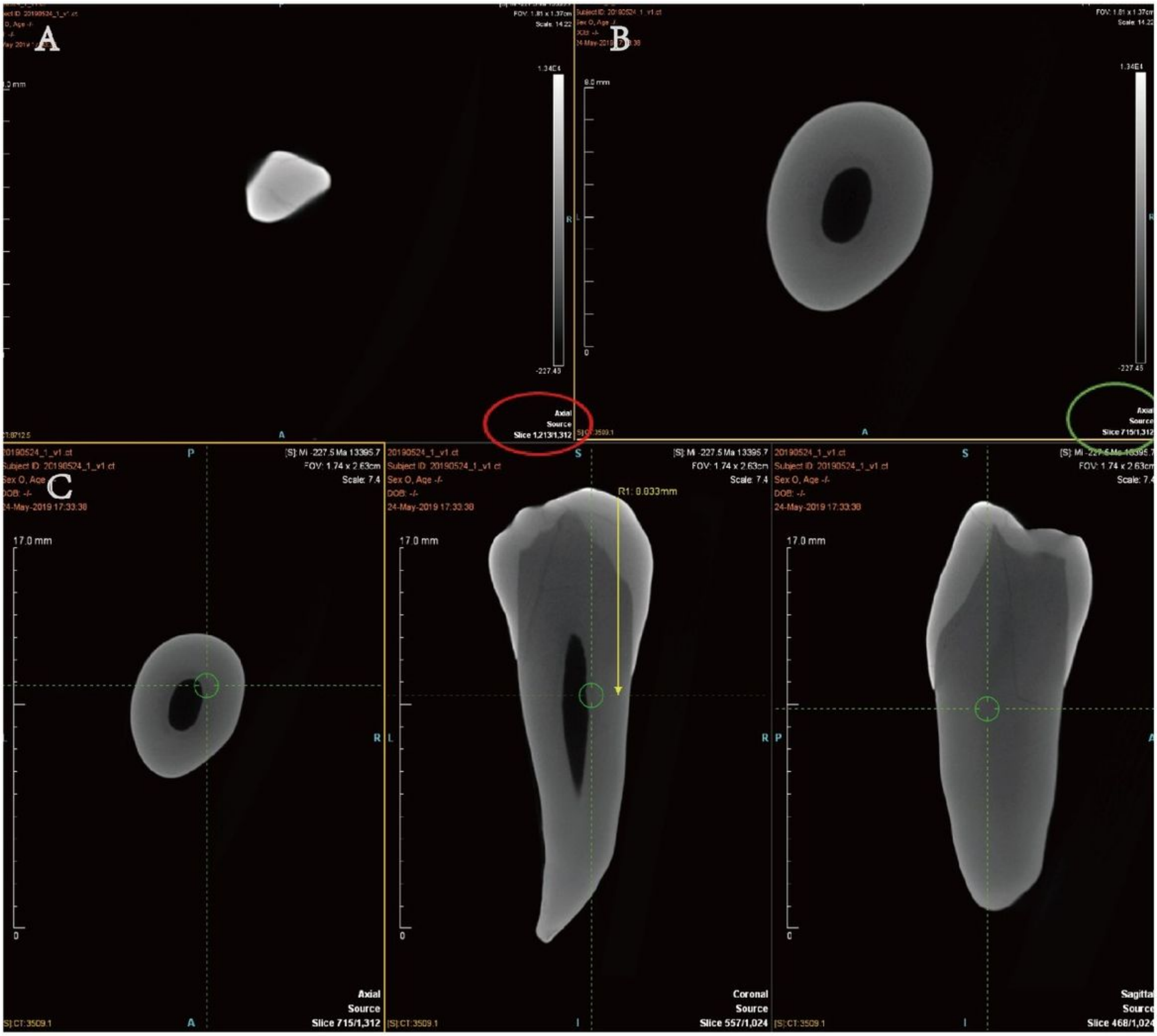

Figure 1

Measurement of the crack depth of a cracked tooth on micro-computed tomography. (A) Appearance of the crown crack on the horizontal plane at layer 1213 (indicated with a red circle); (B) complete disappearance of the root crack at layer 715 (indicated with a green circle); (C) the distance from layer 1213 to layer 715, as measured with the ruler tool, (indicated with a yellow line) is the crack depth; in this case, the depth is 8.833 mm.

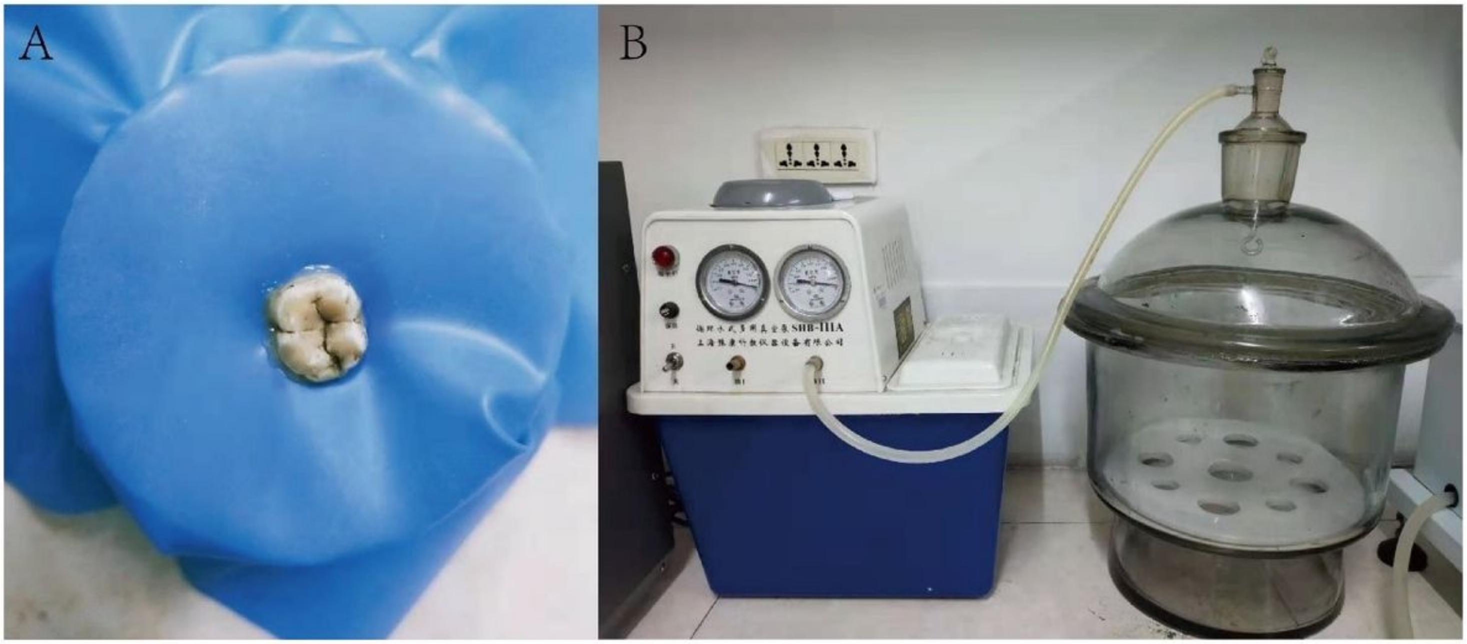

Figure 2

Device used to infiltrate the contrast medium into the crack. (A) The crown of the cracked tooth is exposed with a rubber dam. (B) The closed glass jar and suction pump device are connected to provide negative pressure suction.

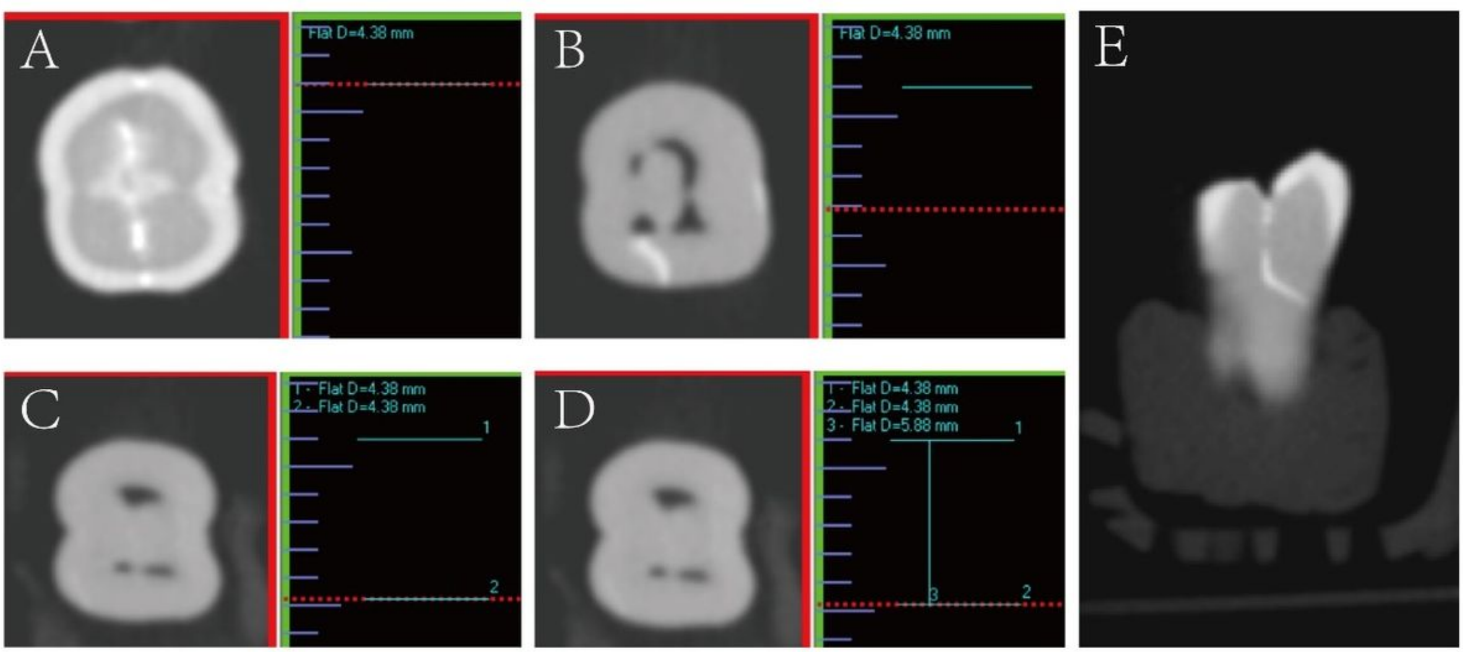

Figure 3

Method of measuring the crack depth of tooth no. 23 on contrast-enhanced cone bean computed tomography (CBCT). (A) The first location where the high-density crack started to appear on the contrast-enhanced CBCT scan is marked “1” at the coronal plane. (B) A high-density crack image of a cracked tooth. (C) The crack completely disappeared and is marked “2”. (D) The distance from “1” to “2”, i.e., the length of segment “3”, was taken as the extension depth of the crack. (E) The coronal plane of the crack shows the path of the crack.

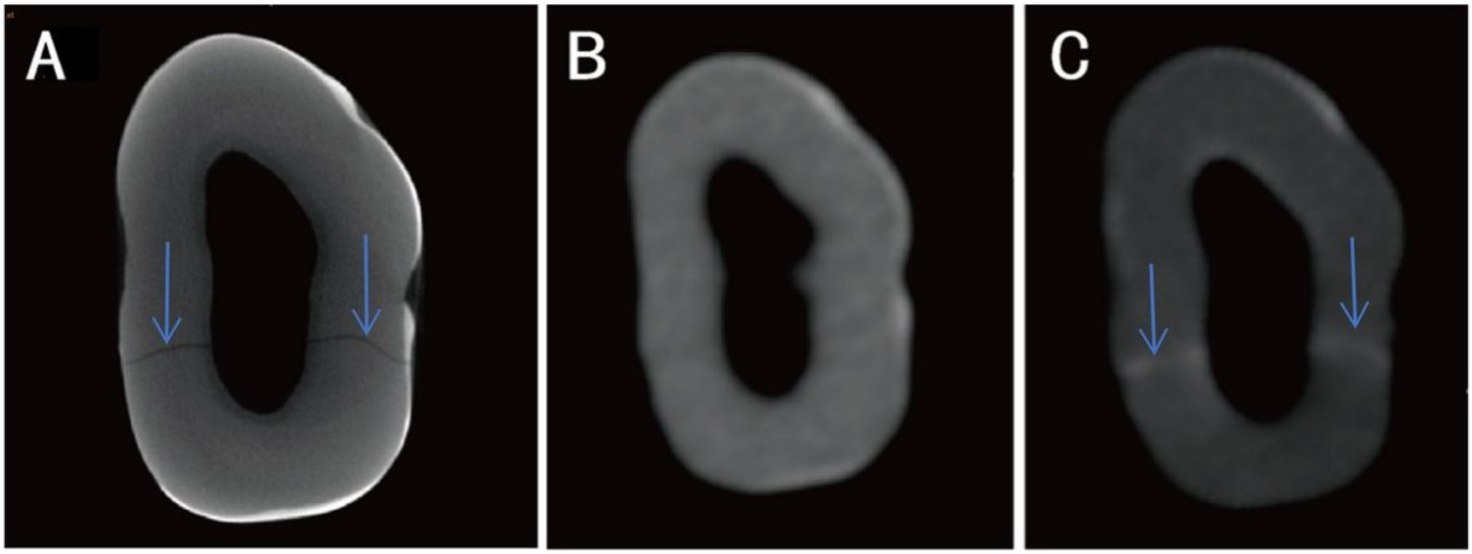

Figure 4

Pre-experimental cone beam computed tomography (pre-CBCT), micro-computed tomography (micro-CT), and contrast-enhanced cone beam computed tomography (CBCT) images of cracked tooth no. 8, which has a mesiodistal crack. (A) Horizontal plane of the crack on micro-CT (the blue arrows indicate the crack). (B) Horizontal plane of the crack on pre-CBCT (showing no crack). (C) Horizontal plane of the crack on contrast-enhanced CBCT (the blue arrow indicates the crack).

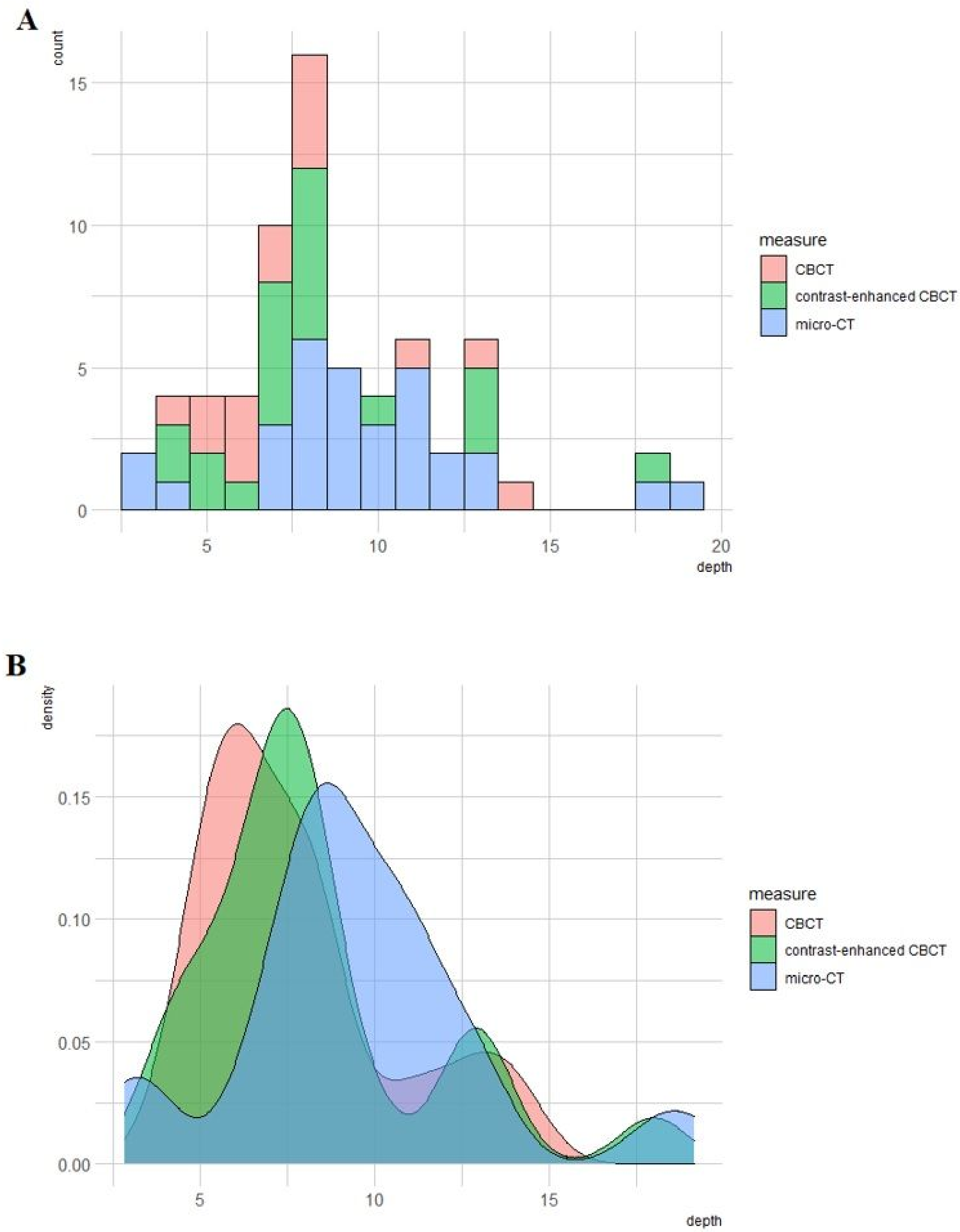

Figure 5

The histogram (A) and the kernel density plot (B) of crack depths measured by pre-CBCT, contrasted-enhanced CBCT and micro-CT.

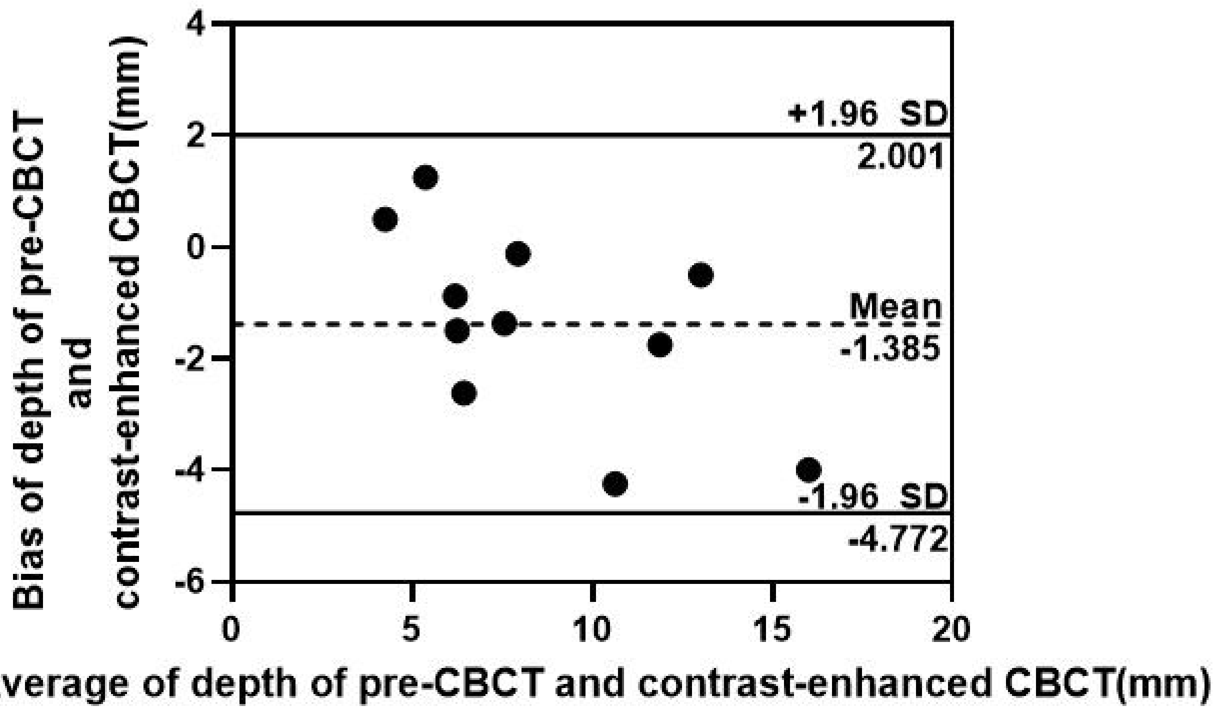

Figure 6

Bland-Altman plot of the crack depths on 11 cracked tooth measured both by pre-CBCT and contrasted-enhanced CBCT, with the representation of the limits of agreement, from -1.96s to +1.96s.

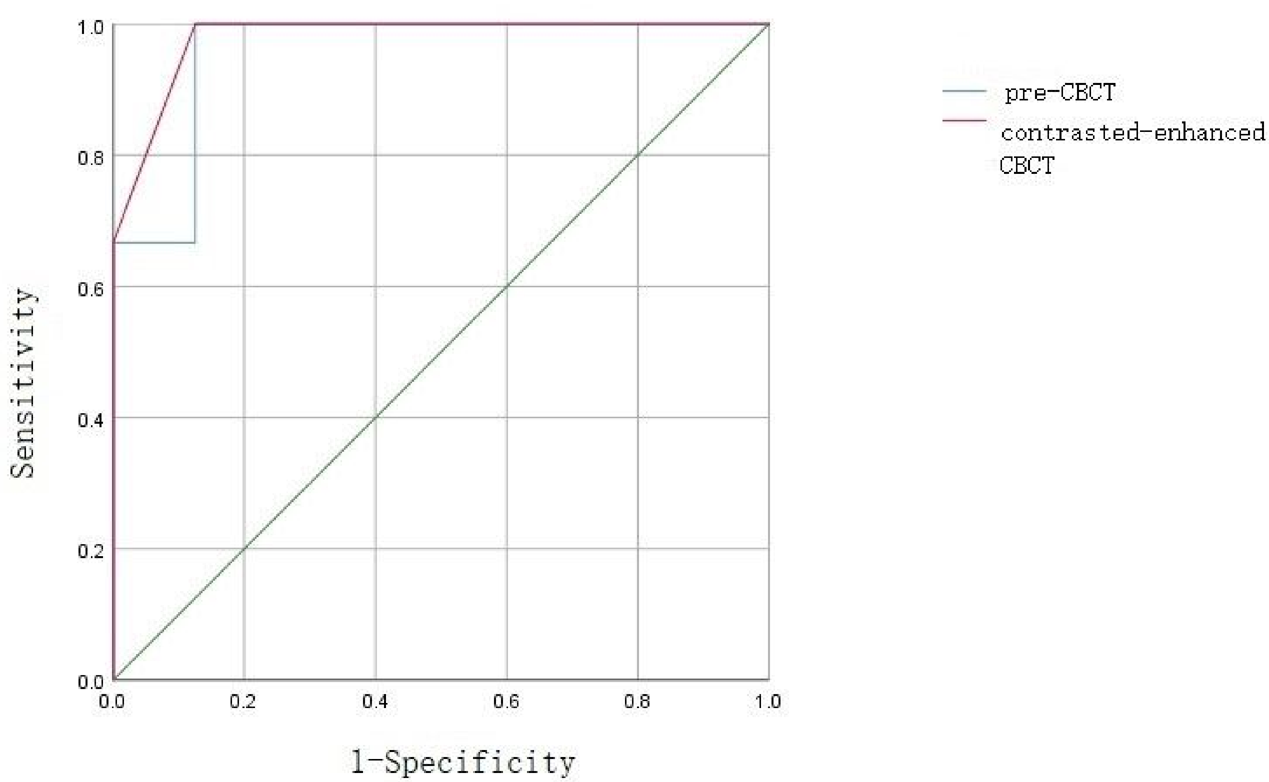

Figure 7

Receiver operating characteristic (ROC) curves of the two measurements. The blue line represents pre-CBCT which had good discriminative power with Area under ROC curve (95% confidence interval) of 0.958 (95% CI: 0.843-1.074). The red line represents contrasted-enhanced CBCT which had good discriminative power with Area under ROC curve (95% confidence interval) of 0.979 (95% CI: 0.921-1.037).

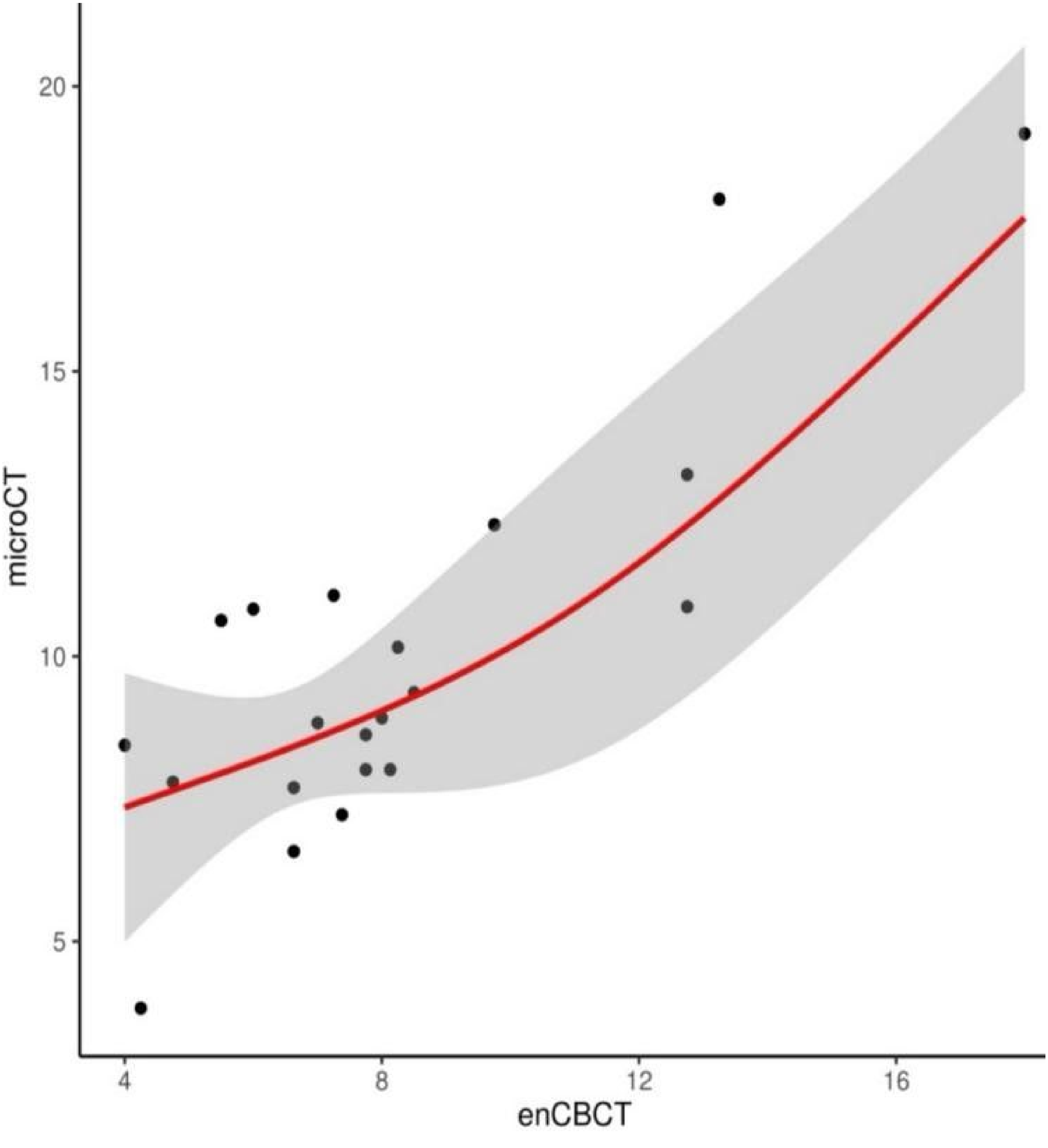

Figure 8

Risk-adjusted, restricted cubic splines with 4 knots of crack depths measured by contrast-enhanced CBCT and crack depths measured by micro-CT. Axis of X was the crack depths measured by contrast-enhanced CBCT; Axis of Y was the crack depths measured by micro-CT. Red line represents crack depths measured by micro-CT; Grey area represents 95% confident interval. Root mean square error (RMSE) was 1.813, R^2 was 0.724, P = 0.000. enCBCT: contrast-enhanced CBCT.